CONF-880280--2

DE88 012530

RESULTS FROM CERN EXPERIMENT WA80

R. Albrecht,[a] T. C. Awes,[b] C. Baktash,[b] P. Beckmann,[c] F. Berger,[c] R. Bock,[a] G. Claesson,[a] L. Dragon,[c] R. L. Ferguson,[b] A. Franz,[d] S. Garpman,[e] R. Glasow,[c] H. A. Gustafsson,[e] H. H. Gutbrod,[a] K. H. Kampert,[c] B. W. Kolb,[a] P. Kristiansson,[d] I. Y. Lee,[b] H. Loehner,[c] I. Lund,[a] F. E. Obenshain,[b] A. Oskarsson,[e] I. Otterlund,[e] T. Peitzmann,[c] S. Persson,[e] F. Plasil,[b] A. M. Poskanzer,[d] M. Purschke,[c] G. Ritter,[d] R. Santo,[c] H. R. Schmidt,[a] T. Siemiarczuk,[a,f] S. P. Sorensen,[b,g] E. Stenlund,[e] and G. R. Young[b]

Presented by H. H. Gutbrod and F. Plasil

— Invited Paper —

International Conference
on Physics and Astrophysics of the Quark-Gluon Plasma,
Bombay, India, February 8-12, 1988

a) Gesellschaft fuer Schwerionenforschung (GSI), D-6100 Darmstadt, West Germany.
b) Oak Ridge National Laboratory,* Oak Ridge, Tennessee 37831.
c) University of Muenster, D-4400 Muenster, West Germany.
d) Lawrence Berkeley Laboratory, Berkeley, California 94720.
e) University of Lund, S-22362 Lund, Sweden.
f) On leave of absence from the Institute of Nuclear Studies, Warsaw, Poland.
g) University of Tennessee, Knoxville, Tennessee 37996.

* Operated by Martin Marietta Energy Systems, Inc., under contract DE-AC05-84OR21400 with the U.S. Department of Energy.

RESULTS FROM CERN EXPERIMENT WA80

R. Albrecht,[a] T. C. Awes,[b] C. Baktash,[b] P. Beckmann,[c] F. Berger,[c] R. Bock,[a] G. Claesson,[a] L. Dragon,[c] R. L. Ferguson,[b] A. Franz,[d] S. Garpman,[e] R. Glasow,[c] H. A. Gustafsson,[e] H. H. Gutbrod,[a] K. H. Kampert,[c] B. W. Kolb,[a] P. Kristiansson,[d] I. Y. Lee,[b] H. Loehner,[c] I. Lund,[a] F. E. Obenshain,[b] A. Oskarsson,[e] I. Otterlund,[e] T. Peitzmann,[c] S. Persson,[e] F. Plasil,[b] A. M. Poskanzer,[d] M. Purschke,[c] H. G. Ritter,[d] R. Santo,[c] H. R. Schmidt,[a] T. Siemiarczuk,[a,f] S. P. Sorensen,[b,g] E. Stenlund,[e] and G. R. Young[b]

Presented by H. H. Gutbrod and F. Plasil

1. INTRODUCTION

As in the case of most of the experiments discussed at this conference, the primary goal of WA80 is a search for evidence that a quark-gluon plasma (QGP) has been formed, or that some similar phase transition has taken place. A number of signatures for QGP formation have been suggested,[1,2] and most experiments have been designed so as to obtain data that pertain to one or more of these signatures. In the case of WA80, the primary probe for the investigation of the QGP is the measurement of photons that may be emitted from the plasma phase. An understanding of the various QGP signatures, however, requires an understanding of the background created by reaction products that do not relate directly to QGP production and thus requires a thorough

---

a) Gesellschaft fuer Schwerionenforschung (GSI), D-6100 Darmstadt, West Germany.
b) Oak Ridge National Laboratory,* Oak Ridge, Tennessee 37831.
c) University of Muenster, D-4400 Muenster, West Germany.
d) Lawrence Berkeley Laboratory, Berkeley, California 94720.
e) University of Lund, S-22362 Lund, Sweden.
f) On leave of absence from the Institute of Nuclear Studies, Warsaw, Poland.
g) University of Tennessee, Knoxville, Tennessee 37996.
* Operated by Martin Marietta Energy Systems, Inc., under contract DE-AC05-84OR21400 with the U.S. Department of Energy.

understanding of the reaction mechanisms governing nucleus-nucleus collisions at these extreme energies. Consequently, another important goal of WA80 is to survey nucleus-nucleus collisions at 60 and 200 GeV/nucleon and to compare the results to those obtained from proton-nucleus interactions. We have pursued this second goal by measuring forward and transverse energies,[3,4] by studying the multiplicities of produced charged particles over a large range of pseudorapidity,[5,6] by investigating transverse momentum spectra of neutral products,[7,8] and by examining target fragmentation products.[9] In this paper we review all of our results obtained with 60- and 200-GeV/nucleon ^{16}O projectiles,[3,4,7-9] with the exception of charged-particle multiplicity data,[5,6] which are discussed in a separate presentation at this conference.[10] We also present the first preliminary calorimeter results from ^{32}S bombardments at 6.4 TeV.

In order to separate characteristic features of nucleus-nucleus collisions, such as collective effects, from those that may be expected on the basis of a superposition of nucleon-nucleon collisions, we compare measured quantities with results of calculations that reproduce data from nucleon-induced reactions and that make predictions for nucleus-nucleus collisions. Several models are available for such comparisons. Unfortunately, the advantages and disadvantages of the various models have not, as yet, been investigated in a systematic manner. Thus, a comparison of the various physical ingredients, of limitations, and of the degree to which the models describe the increasing volume of data is a matter of high priority. In this paper, we make comparisons with FRITIOF,[11] which is a nucleus-nucleus version of the LUND model. Effects of detector acceptance and of trigger bias are included in all FRITIOF calculations.

2. EXPERIMENTAL APPARATUS

The experimental setup has been described previously.[12,13] A schematic drawing of all WA80 components is shown elsewhere in these proceedings.[10] In Fig. 1, for the purpose of clarity, we show only the detectors which were used to obtain the data presented here. These are the Mid-Rapidity Calorimeter (MIRAC), the Zero-Degree Calorimeter

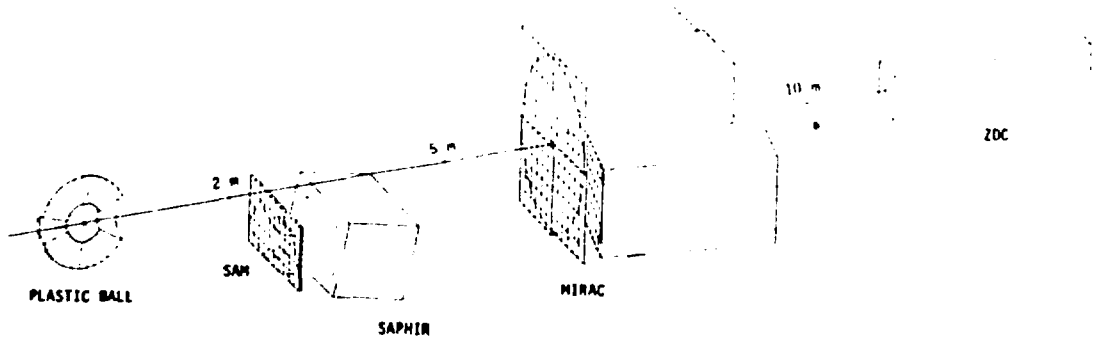

Fig. 1. Components of the WA80 experimental arrangement discussed in this work. MIRAC and ZDC are the Mid-Rapidity and the Zero-Degree Calorimeters, respectively. SAPHIR is the lead-glass photon detector, and SAM is the multiplicity array used to identify charged particles incident on SAPHIR. The target is at the center of the Plastic Ball.

(ZDC), the Plastic Ball, and SAPHIR, the finely-segmented single-arm photon detector. Both MIRAC and the ZDC are metal-scintillator sampling calorimeters with separate electromagnetic and hadronic readouts. MIRAC is divided into 20 x 20 cm^2 towers located at 6.5 m from the target and provides full azimuthal coverage in a pseudorapidity (η) range from 2.4 to 5.5, with partial coverage extending down to $\eta = 2.0$. Further MIRAC coverage is provided for approximately 10% of azimuthal angles in the range $1.6 \lesssim \eta \lesssim 2.4$. The measured σ/E resolutions of MIRAC are 14.2% for 10-GeV/c charged pions, and 5.1% for 10-GeV/c electrons. The ZDC measures the total energy of projectile spectators and leading particles that pass through a beam hole in MIRAC. This hole has an inscribed cone angle of 0.3°, corresponding to $\eta > 6.0$. The resolution of the ZDC was measured to be 2.5% at 3.2 TeV and 4.5% at 0.96 TeV.

Inclusive photon and π^0 distributions are measured by the electromagnetic calorimeter SAPHIR. It consists of 1278 lead-glass modules and covers a solid angle of 0.13 sr in the range $1.5 < \eta < 2.1$. Its measured σ/E resolution is given by $(6/\sqrt{E/GeV} + 0.4)\%$. Background from charged-particles is greatly reduced by means of a double layer of plastic streamer tubes located in front of SAPHIR, resulting in a 98% charged-particle detection probability. The π^0 reconstruction efficiency rises from 20-30% at low (0.2-0.3 GeV/c) values of the pion

transverse momentum, p_T, to 80-90% at 2-6 GeV/c. The π^0 mass resolution is in the range of 5-8%. For SAPHIR measurements, a low-background environment is particularly important to minimize the extent of photon conversion. Care was taken to keep all extraneous material out of the reaction zone, and background levels during target-out operation were found to be negligible. In addition, thin targets were used to minimize contributions from secondary interactions. During ^{16}O bombardments, the target thicknesses were 186 mg cm^{-2} of C and 250 mg cm^{-2} of Au, corresponding to average photon conversion probabilities of 0.2% and 1.6%, respectively.

A unique capability for the study of charged-particle target remnants is provided by the Plastic Ball.[14] It covers an angular range of 30° to 160° ($-1.7 < \eta < 1.3$) and consists of 655 ΔE-E modules, each capable of identifying and of measuring the energy of charged pions, protons, deuterons, tritons, and $^{3,4}He$. Above 400 MeV, protons cannot be separated from charged pions, and corrections are made to take this into account. Corrections are also made for multiple hits in single detector modules. For central collisions of O + Au, the number of multiple hits is as high as 40% in the forward-most modules.[9] The multiple-hit corrections integrated over the whole Plastic Ball range from about 18% for central O + Au collisions (10% for minimum-bias events) to negligible values for O + Cu and O + C collisions.

In the following sections we describe, in turn, forward and transverse energy measurements and such related quantities as nuclear stopping and energy densities, transverse momentum spectra of neutral products, and target fragmentation results.

3. ZDC ENERGY DISTRIBUTIONS

An important aspect of high-energy nucleus-nucleus collisions is the nuclear collision geometry[3,4,15] as determined by the relative sizes of the target and projectile nuclei, the overlap volume in the collision, and the impact parameter. As a consequence, simple geometrical considerations can be used as a key for a qualitative understanding of the ZDC energy spectra shown in Fig. 2 for ^{16}O-induced reactions

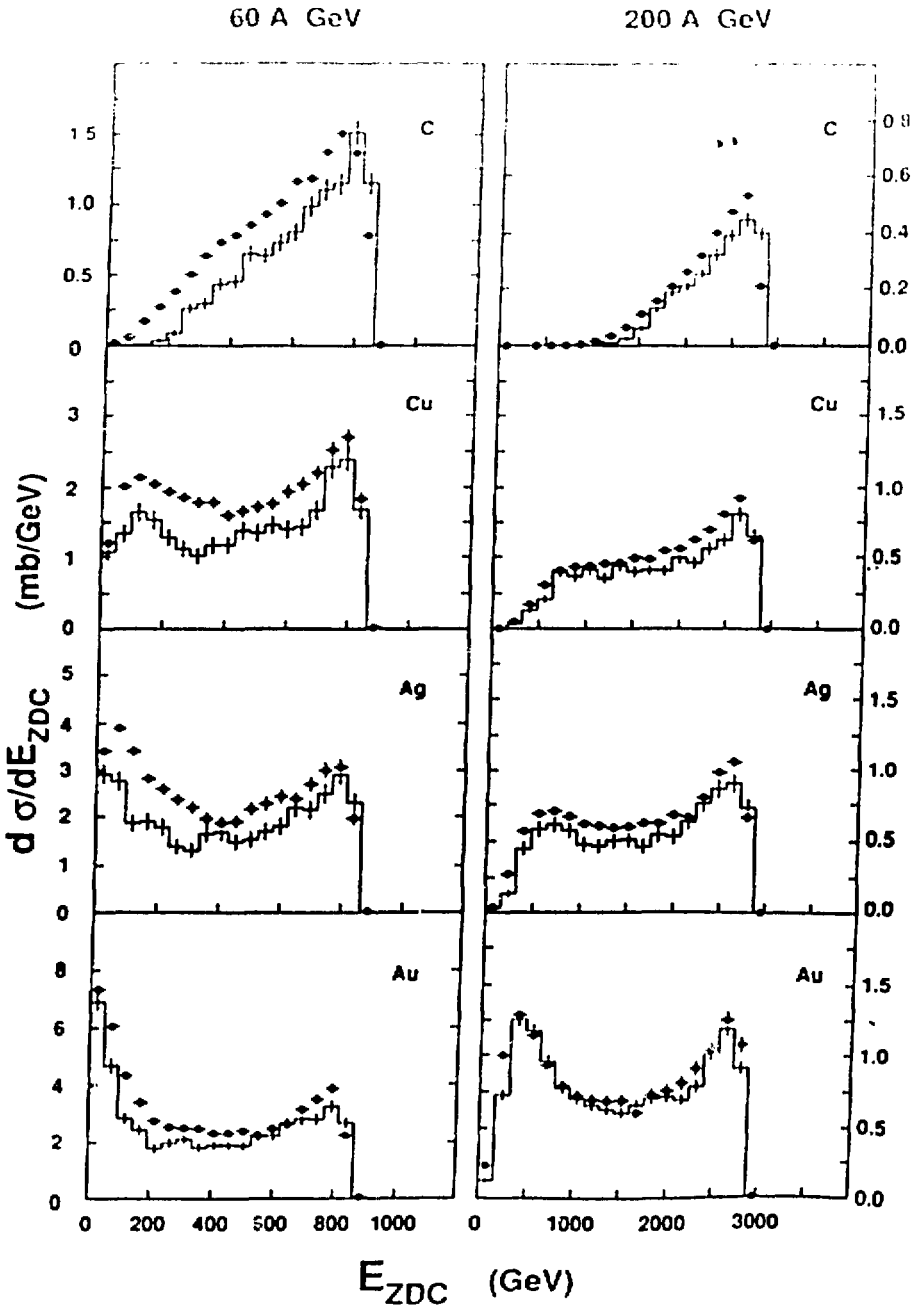

Fig. 2. Energy Spectra measured in the Zero-Degree Calorimeter (filled circles) in ^{16}O-induced reactions. Histograms give the results of FRITIOF calculations.[11] The vertical error bars represent statistical errors.

and in Fig. 3 for ^{32}S reactions. At 200 A GeV, the $^{16}O + ^{12}C$ and the $^{32}S + ^{27}Al$ reactions have essentially no cross section for events

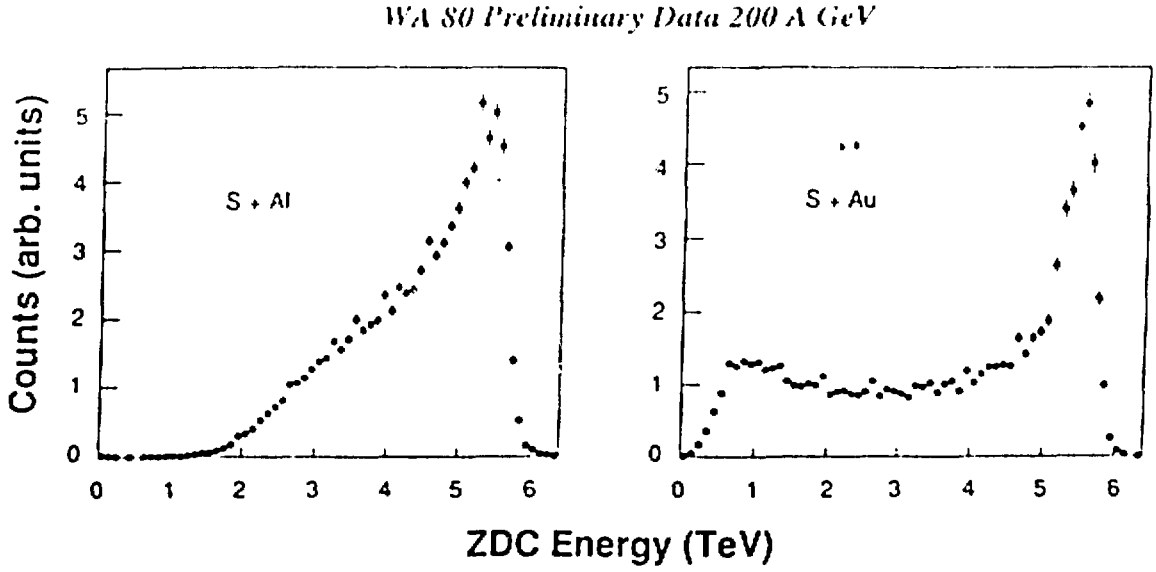

Fig. 3. Preliminary ZDC spectra from ^{32}S reactions with Al and Au at 200 A GeV.

depositing a small amount of energy in the ZDC because, in a simple participant spectator picture, even in the most central collisions, several projectile spectator nucleons, each with an energy of 200 GeV, proceed in the beam direction. In contrast, a pronounced peak is seen at small ZDC energies in the spectrum from the $^{16}O + ^{197}Au$ reaction and, to a lesser degreee, in the $^{32}S + ^{197}Au$ spectrum. In these cases, events with low ZDC energies result from central collisions in which the smaller projectile nuclei are embedded in the massive Au target nuclei, resulting in the emission of only a few leading particles at angles less than 0.3°. Furthermore, in these cases, a wide range of impact parameters gives rise to collisions in which the entire projectile interacts with a nearly constant number of target nucleons, thus producing the peak at low ZDC energies.

In Fig. 2 the effects of the more restricted acceptance of the ZDC at 60 A GeV, as compared to the acceptance at 200 A GeV, are clearly seen. The peak at the lowest energies in the 60 A GeV $^{16}O + ^{197}Au$ spectrum is even more pronounced than it is at the higher bombarding energy. Furthermore, in the 60 A GeV $^{16}O + ^{12}C$ reaction,

there are many more events with low ZDC energies, as compared to the 200 A GeV case. These events probably originate from collisions in which one or more of the projectile spectator fragmentation products have pseudorapidities that are low enough for them to be intercepted by MIRAC.

FRITIOF model calculations are shown as histograms in Fig. 2. The agreement with the data is better at 200 A GeV than at 60 A GeV, where there is a tendency for FRITIOF to underestimate the cross sections at small ZDC energy values, especially for the lighter targets. This discrepancy may be caused in part by effects of projectile spectator fragmentation, which are not included in FRITIOF. Furthermore, the calculations depend on the particular nuclear density prescription used in the model.[3,4] The overall general agreement, however, indicates that the model provides a reasonable description of the impact-parameter dependence of longitudinal momentum transfer.

4. TRANSVERSE ENERGY DISTRIBUTIONS

Measurements of transverse energies are important since they provide a basis for estimates of the degree of nuclear stopping and of the magnitude of attained energy densities. The transverse energy produced is measured on an event-by-event basis in MIRAC and is calculated as $E_T = \Sigma E_i \sin(\theta_i)$, where E_i and θ_i are the observed energy and the effective angle of each element i of MIRAC, respectively. The transverse energy distributions for $2.4 < \eta < 5.5$ are shown as filled circles in Fig. 4. As in the case of the ZDC spectra, the shapes of the E_T spectra are dominated by effects of the nuclear collision geometry. The spectra for the heaviest nuclei, Ag and Au, show a large "plateau" extending out to 80-100 GeV at 200 A GeV beam energy and to 40-45 GeV at 60 A GeV. The Au spectra have a broad peak at the high-energy end of the plateau. This peak is closely correlated with the low-energy peak in the ZDC spectra for Au[3]. This correlation demonstrates that the peak in the E_T distribution, corresponding to low ZDC energies, originates from the most central collisions, in which the entire projectile interacts with a nearly constant number of target nucleons. As the target becomes

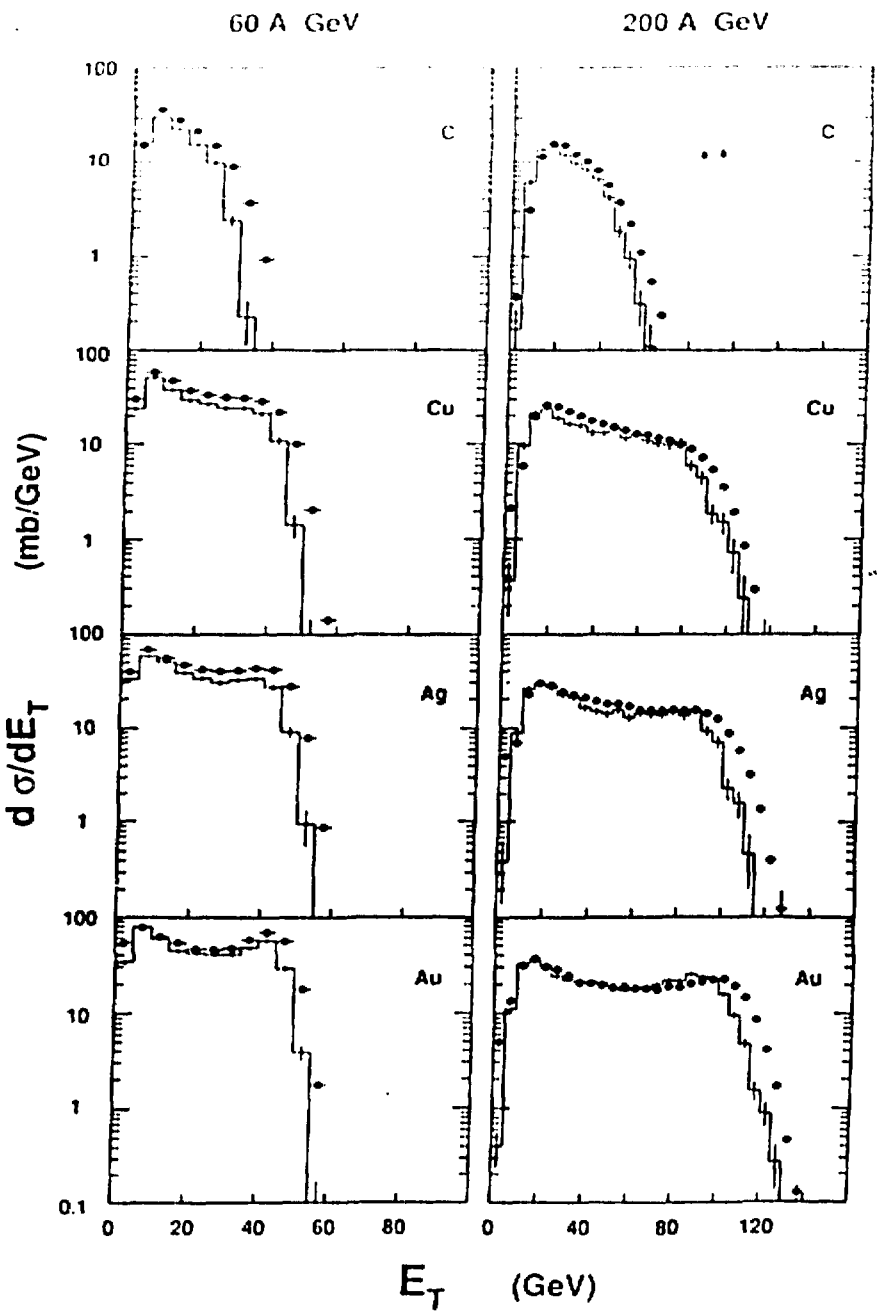

Fig. 4. Transverse energy distributions measured in the pseudorapidity range of $2.4 < \eta < 5.5$ for 60 A GeV and 200 A GeV ^{16}O projectiles incident on targets of C, Cu, Ag, and Au. The experimental results (filled circles) are presented with their statistical errors. Histograms give the results of FRITIOF calculations.[11]

smaller, the peak and the plateau become less pronounced. For $^{16}O + ^{12}C$, the E_T spectra have shapes similar to those of the E_T spectra measured in proton-induced reactions[16], while the spectra from $^{16}O + ^{197}Au$ reactions are similar to the E_T spectra from ^{16}O + Pb reactions obtained by the NA35 collaboration[15].

At 60 A GeV the high-energy tails of the E_T distributions for Cu, Ag, and Au targets almost coincide with one another at a value of approximately 60 GeV. This phenomenom could be caused by "complete stopping," as discussed by the E802 collaboration for data obtained at 15 A GeV.[17] However, at our beam energies, this finding is more likely to be due to a combination of two opposing effects. As the target mass or number of target participants increases, the maximum transverse energy increases. At the same time, however, the rapidity of the effective c.m. system decreases, leading to decreased coverage by MIRAC. At 60 A GeV these two effects tend to cancel each other; whereas, at 200 A GeV, the increase in E_T dominates over the decreasing coverage, resulting in a net increase of the observed transverse energy. This demonstrates that the precise shapes of the observed E_T spectra are a sensitive function of the pseudorapidity region in which they are measured. Thus, in measurements with coverage of the lower pseudorapidity region, no peak has been seen at high E_T for heavy targets[18]. FRITIOF calculations are consistent with this observation.

The histograms in Fig. 4 are the results of FRITIOF calculations. At both bombarding energies, the model gives a good description of the shapes of the E_T spectra, but consistently underestimates the transverse energy scale in the tail region by 10% to 15%.

Preliminary transverse energy spectra for 200 A GeV ^{32}S projectiles incident on ^{27}Al and ^{197}Au target nuclei are shown in Fig. 5. Also shown for comparison is the transverse energy distribution for $^{16}O + ^{197}Au$ with the same preliminary calibration. It can be seen that the transverse energy for central events is about 60 to 70% higher for $^{32}S + ^{197}Au$ than for $^{16}O + ^{197}Au$. The magnitude of this increase scales with the number of participants involved, as is seen in the next section.

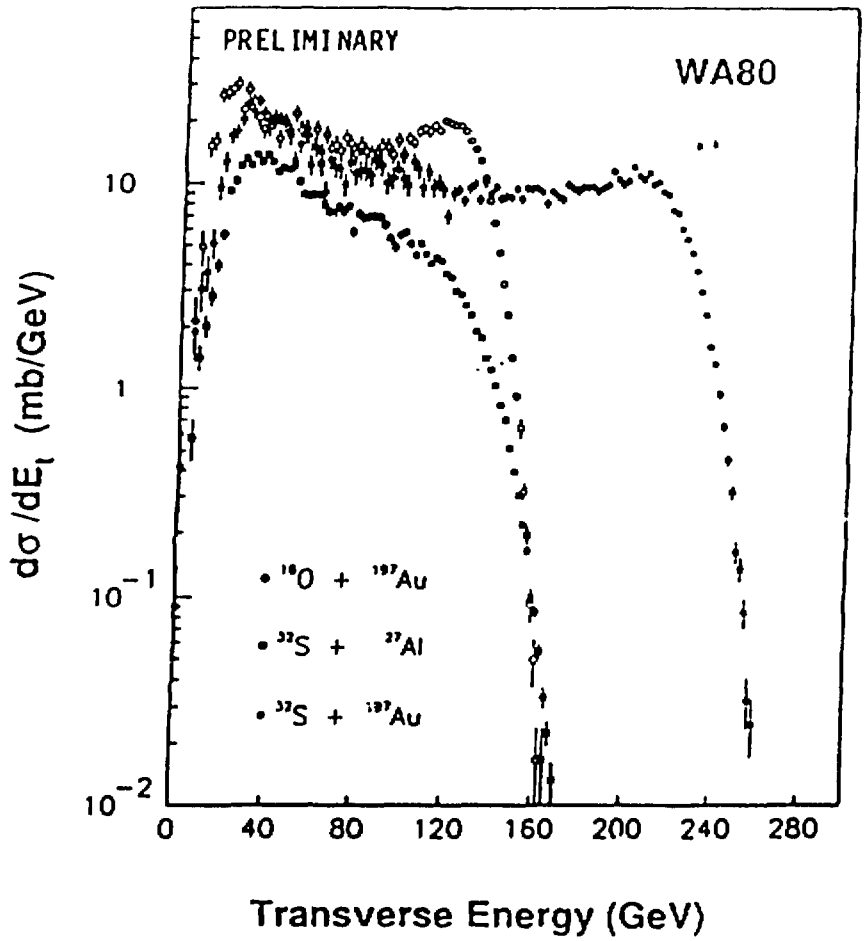

Fig. 5. Preliminary transverse energy distributions measured in the pseudorapidity range of $2.4 < \eta < 5.5$ for 200 A GeV ^{32}S on targets of Al and Au. Also shown for comparison is the ^{16}O on Au result with the same preliminary calibration.

5. NUMBER OF PARTICIPANTS

In this section we present simple relationships between the impact parameter, the ZDC energy, the number of participants, and the average transverse energy per participant. Two alternative methods have been used to obtain estimates of the average number of participating nucleons as a function of measured ZDC energy. The first method relies on the agreement between FRITIOF predictions and measured ZDC spectra. It makes use of the model to establish a relationship between ZDC energies and the calculated number of participants. The second method assumes a

monotonic increase of the impact parameter with ZDC energy and makes use of the relationship between impact parameter and the absolute cross section obtained from a sharp sphere nuclear shape model. The two methods give nearly identical results.[3]

Since a relationship between the total number of participants and the ZDC energy has been established, the E_T distributions can be examined as a function of the number of participating nucleons. In Fig. 6, the average E_T per participant is shown as a function of the ZDC energy. This $\langle E_T/\text{participant}\rangle$ is calculated using the azimuthal-acceptance-corrected E_T measured in the pseudorapidity interval $1.6 < \eta < 5.5$ and the average number of participants corresponding to the observed ZDC energy. The striking feature of Fig. 6 is that, at a given bombarding energy, the $\langle E_T/\text{participant}\rangle$ remains nearly constant as a function of target mass and decreases only slowly with decreasing collision centrality.

It is interesting to note that for central collisions (lowest ZDC energies) the number of participants is 68 for ^{16}O + Au and 115 for ^{32}S + Au, respectively. The ratio of these two numbers is approximately equal to the ratio of the central-collision transverse energies produced in the two reactions (see Fig. 5).

6. NUCLEAR STOPPING

In the absence of a precise definition of "nuclear stopping," we present results in terms of two ratios, S_{int} and S_{mid}, between measured and calculated values of transverse energies. First, we estimate the maximum value of transverse energy, E_T^{max}, under the assumptions that (a) in central collisions all the projectile nucleons react with a cylinder of the target nucleus that has a base area equal to the cross section of the projectile; and (b) all of the available center-of-mass energy, E'_{CM}, is emitted isotropically in the CM system. E'_{CM} is obtained from the CM energy by subtracting the rest mass of the participating baryons. In this simple model $E_T^{max} = (\pi/4)E'_{CM}$, and the ratio S_{int} is defined as E_T^{int}/E_T^{max}, where E_T^{int} is the integral of a Gaussian distribution fitted to the experimental $dE_T/d\eta$ distribution in the range

$1.6 < \eta < 5.5$. Similarly, S_{mid} is defined as the ratio of the maximum value of the experimental $dE_T/d\eta$ distribution (the maximum value of the

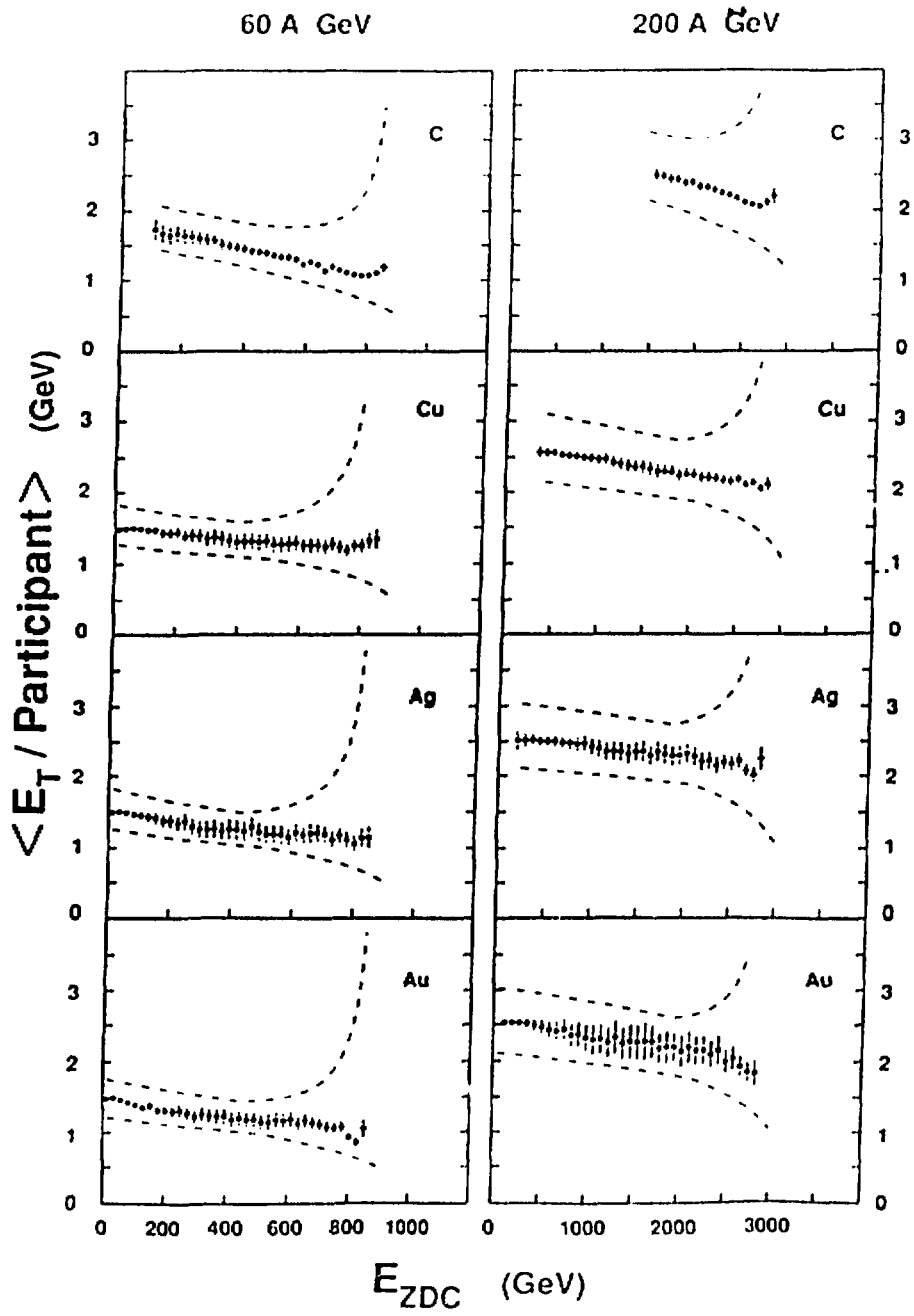

Fig. 6. Average values of E_T/participant as a function of the energy measured in the Zero-Degree Calorimeter. The pseudo-rapidity range used in the E_T determination is $1.6 < \eta < 5.5$. The dashed lines indicate the estimated limits of systematic errors.

fitted Gaussian) to the maximum value of the calculated $dE_T/d\eta$ distribution, which is given by 0.5 E'_{CM}. For ^{16}O + ^{197}Au the integral ratio, S_{int}, is found to be 57 ± 9% at 60 A GeV and 51 ± 8% at 200 A GeV. The mid-rapidity ratio, S_{mid}, varies from 34 ± 4% and 27 ± 3% for ^{16}O + ^{197}Au at the lower and higher bombarding energy, respectively, to 31 ± 3% and 21 ± 2% for the ^{16}O + ^{12}C reaction. The target dependence of nuclear stopping is, thus, found to be weak; and the degree of stopping in the ^{16}O + ^{197}Au case is estimated to lie between 25 and 60 percent.

7. ENERGY DENSITIES

Theoretical predictions for possible QGP formation are usually given in terms of energy densities required for plasma formation to take place. Thus, estimates of attained energy densities derived from nucleus-nucleus collision data are of great interest. Unfortunately, no generally accepted method exists for the determination of the energy density, ε, from experimental results. In this work we estimate ε using three different approaches.

In the first method ε is estimated using the following formula, based on an expression first suggested by Bjorken[19],

$$\varepsilon_{BJ} = \frac{1}{\tau_0 \pi R_p^2} \left.\frac{dE}{dy}\right|_{y=y_{c.m.}},$$

where R_p is the radius of the projectile, the initial formation time τ_0 is taken to be 1 fm/c, and the transverse area of the interaction region is calculated with a radius parameter r_0 of 1.2 fm. The energy content of the volume $\tau_0 \pi R_p^2$ is usually evaluated as

$$\left.\frac{dE}{dy}\right|_{y=y_{c.m.}} = f \cdot \left.\frac{dE_T}{d\eta}\right|_{\eta=\eta_{max}},$$

where the factor f accounts for the partition of the radiated energy between longitudinal and transverse degrees of freedom and is usually assumed to be equal to 1.0. The resulting energy densities for 200 A GeV oxygen interactions with each of the four targets are listed

in Table I. The values for central collisions are observed to increase with increasing target mass from about 1.0 GeV/fm^3 for $^{16}O + ^{27}Al$ to 2.3 GeV/fm^3 for $^{16}O + ^{197}Au$.

The above expression for ε_{BJ} was derived for the extreme relativistic limit in which the observables are boost independent with the rapidity distributions exhibiting a plateau. At the energy considered here, however, this condition is not satisfied, and the following alternative method used to estimate ε is not subject to it. In this approach, ε_{Therm} is deduced from $\varepsilon_{Therm} = E_{Therm}/V$, where E_{Therm} is the total energy thermalized in the center of mass and V is the appropriate volume containing E_{Therm}. E_{Therm} is obtained from the integrated E_T distributions, assuming isotropic radiation in the center of mass. Thus,

$$E_{Therm} = \frac{4}{\pi} E_T^{total} .$$

A conservative estimate for V is obtained on the assumption that E_{Therm} is localized in a volume given by the overlap cylinder at a time after collisions and particle production have ceased. Hence,

$$V = \pi R_p^2 [2(R_p + R_T)/\gamma_{cm} + \tau_0] ,$$

where R_T is the target radius and γ_{cm} takes the Lorentz contraction into account. τ_0 is again taken to be 1 fm/c. Values of ε_{Therm} are also given in Table I. For the heavy systems, they are somewhat lower than ε_{BJ} and vary only slowly with target mass.

In both of the above estimates of ε, *volume-averaged* energy densities have been considered. Since the transverse energy generated has been shown to scale with the number of participants and since the active volume also scales approximately with the number of participants, it is not surprising that the target-projectile dependence of the volume-averaged energy density is weak. The advantage to be attained with systems of increasing mass is the generation of larger active volumes and of higher energy densities in the central core of the overlap volume, as the following discussion demonstrates.

For central collisions at 200 A GeV, our data show that $[dE_T/d\eta]_{max}$ scales approximately with the number of participants, W, with a factor of proportionality close to 1 GeV/nucleon; i.e.,

$$\frac{d^2E_T}{d\eta dW} = 1 \text{ GeV/nucleon (central collisions)} .$$

Along the symmetry axis in a central collision, the total number of participants per unit transverse area is

$$\frac{dW}{dA_\perp}_{R=0} = 2\rho_0 r_0 (A_p^{1/3} + A_t^{1/3}) .$$

The energy density in the central core, ε_{core}, is, therefore, given approximately by:

$$\varepsilon_{core} = \frac{f}{\tau_0} \frac{d^2E_T}{d\eta dW} \frac{dW}{dA_\perp}_{R=0}$$

$$= 0.38 \ (A_p^{1/3} + A_t^{1/3}) \ [\text{GeV/fm}^3] ,$$

where the following numerical values have been used: $\rho_0 = 0.16$ fm^{-3}, $r_0 = 1.20$ fm, $f = 1$, and $\tau_0 = 1$ fm/c. It should be noted that the above expression implies a significant increase of ε_{core} with increasing projectile size. ε_{core} values are also given in Table I.

Table I. Energy densities, E, in GeV/fm^3. See the text for definitions of ε denoted by the subscripts.

System	ε_{BJ}	ε_{Therm}	ε_{core}
$^{16}O + {}^{12}C$	1.0	1.9	1.8
$^{16}O + {}^{65}Cu$	1.8	2.2	2.4
$^{16}O + {}^{108}Ag$	2.0	2.1	2.7
$^{16}O + {}^{197}Au$	2.3	2.0	3.1
$^{32}S + {}^{197}Au$*	2.4	2.3	3.3
$^{208}Pb + {}^{208}Pb$*	2.5	2.4	4.5

*Energies estimated by scaling $^{16}O + {}^{197}Au$ results with the number of participants.

8. TRANSVERSE MOMENTUM DISTRIBUTION OF PHOTONS

Following the discussion of global reaction characteristics in the preceding sections, we now focus on specific aspects of the reactions in a restricted range of rapidity. In this section we present transverse momentum, p_T, distributions of photons[7,8] measured in the range $1.5 < \eta < 2.1$ with the electromagnetic calorimeter SAPHIR. As was stated in the introduction, the main goal of SAPHIR is to obtain spectra of direct photons. These are obtained by subtracting the large contributions due to π^0 and η decay from the measured inclusive photon distributions. Recently, we have obtained first estimates of direct photon spectra, but they are too preliminary to be presented here. Distributions of reconstructed π^0 events are also of interest and have been discussed elsewhere.[7,8] Here we consider only inclusive spectra of photons, which are dominated by photons originating from π^0 decay, but which comprise SAPHIR data of the highest statistical significance.

Inclusive photon p_T distributions from central events (about 10% of the minimum bias cross section) are shown in Fig. 7. The data can be represented for $p_T > 0.4$ GeV/c by an exponential parametrization,

$$\frac{dN}{dp_T} \sim \exp \frac{-p_T}{T_{eff}} .$$

The slope parameters, T_{eff}, are given in Table II. T_{eff} is seen to increase slightly with increasing target mass, increasing projectile mass, and increasing incident energy. FRITIOF calculations for 200 A GeV $^{16}O + ^{197}Au$ are also shown in Fig. 7. The calculated slope parameter is about 20% lower than that obtained from the data. Similar discrepancies between FRITIOF results and data are also observed for other combinations of target, projectile, and bombarding energy.

The dependence of the p_T distributions on collision centrality is illustrated in Fig. 8, where the ratio of the cross section for high charged-particle multiplicity events to that for low multiplicity events is plotted as a function of p_T. The high and low multiplicity samples comprise about 30% of the most central and of the most peripheral reactions, respectively. The ratios shown in Fig. 8 increase by a factor of 2 for the ^{16}O + Au data in the range 0.5 GeV/c $< p_T <$ 1.5 GeV/c,

while they stay nearly constant for p + Au. This pattern indicates that large transverse momenta are more likely to be produced in violent ^{16}O + Au collisions than in proton-induced reactions. No change in p_T distributions as a function of event centrality" is expected from FRITIOF calculations for any of the systems investigated.

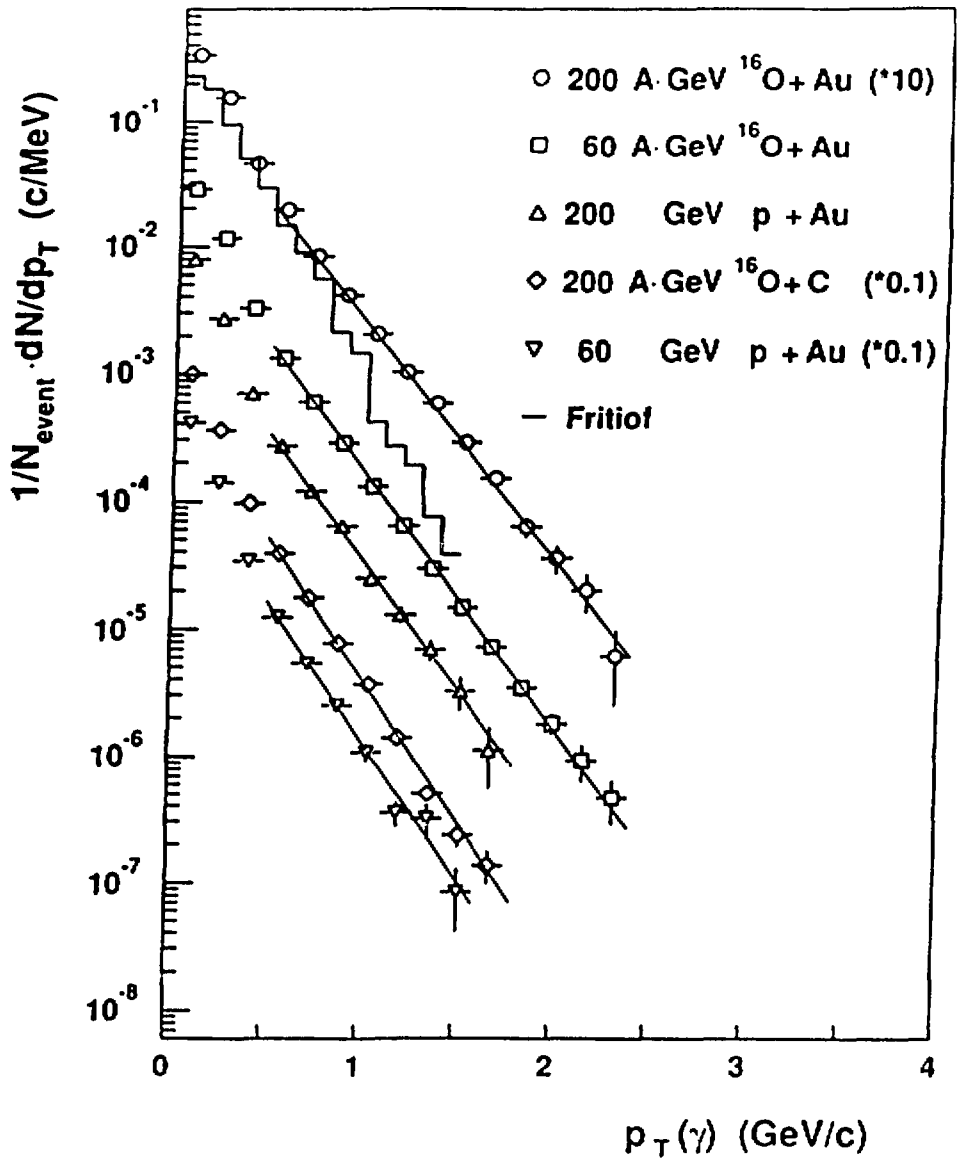

Fig. 7. Inclusive distributions of the transverse momenta of photons from central collisions. Solid lines indicate exponential parametrizations (see text). FRITIOF results[11] are given by histograms for the 200 A GeV ^{16}O + Au case.

Table II. Slope parameters T_{eff} in MeV/c

Bombarding energy	p + Au	^{16}O + C	^{16}O + Au
60 GeV per nucleon	198 ± 3	181 ± 2	215 ± 2
200 GeV per nucleon	215 ± 4	193 ± 3	234 ± 2

Event centrality can also be determined by the Zero-Degree Calorimeter, and, in the discussion below, we consider average transverse momentum values evaluated for $p_T > 400$ MeV/c, $\langle p_T \rangle_{\gamma,400}$, as a function of ZDC energy. Values of $\langle p_T \rangle_{\gamma,400}$ were obtained by fitting exponentials to the p_T distributions and also by calculating averages

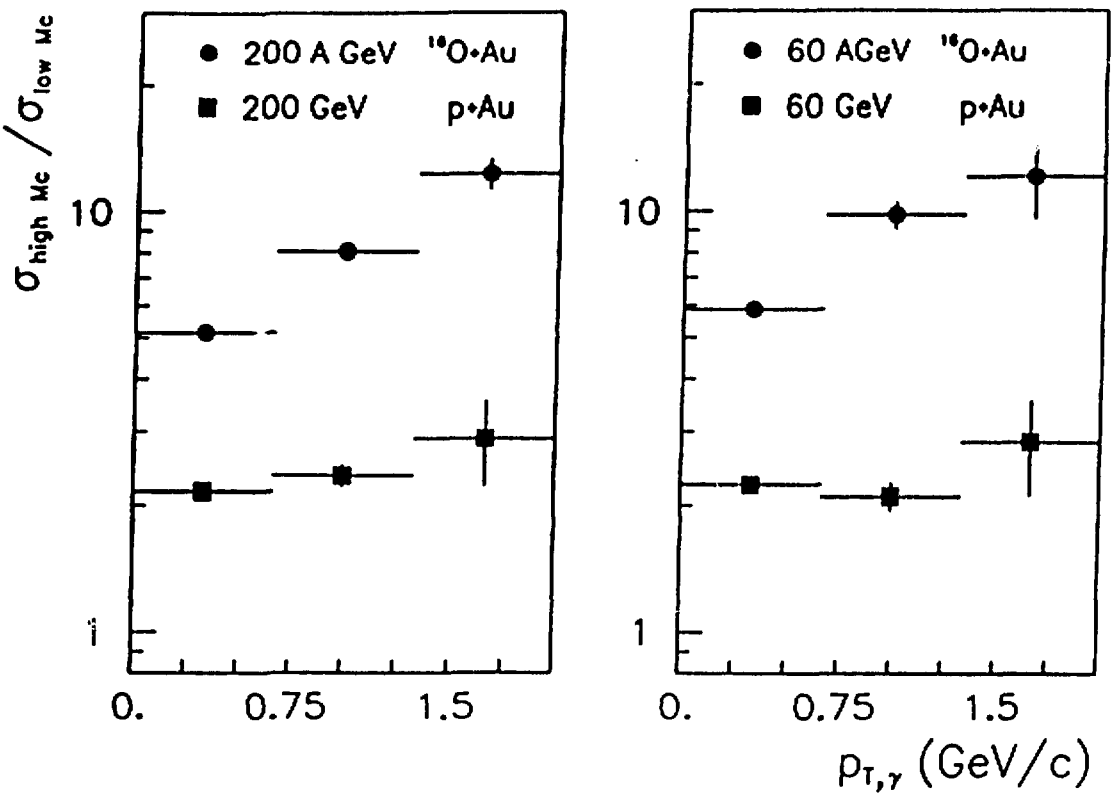

Fig. 8. Ratios of inclusive photon cross sections for high and low charged-particle multiplicity events in ^{16}O + Au and p + Au reactions. The high and low multiplicity selections contain about 30% of the most central and 30% of the most peripheral reactions, respectively.

of truncated distributions. The two methods give nearly identical results. $\langle p_T \rangle_{\gamma,400}$ values obtained with the truncation method are shown in Fig. 9 as a function of the ratio of E_{ZDC} to the beam energy. For the ^{16}O-induced reactions, a 15% decrease in the average transverse momentum is observed with decreasing collision centrality. No obvious trend is apparent in the case of the proton-induced reactions, even when other measures of centrality (charged-particle multiplicities) are considered. FRITIOF results for $\langle p_T \rangle_{\gamma,400}$ are also shown in Fig. 9. The calculations exhibit no variation with centrality or target mass. This discrepancy between data and the LUND model does not depend on the precise position of the truncation cut. The cause of the discrepancy is not understood, and the extent of it may decrease when hard scattering is included in FRITIOF.

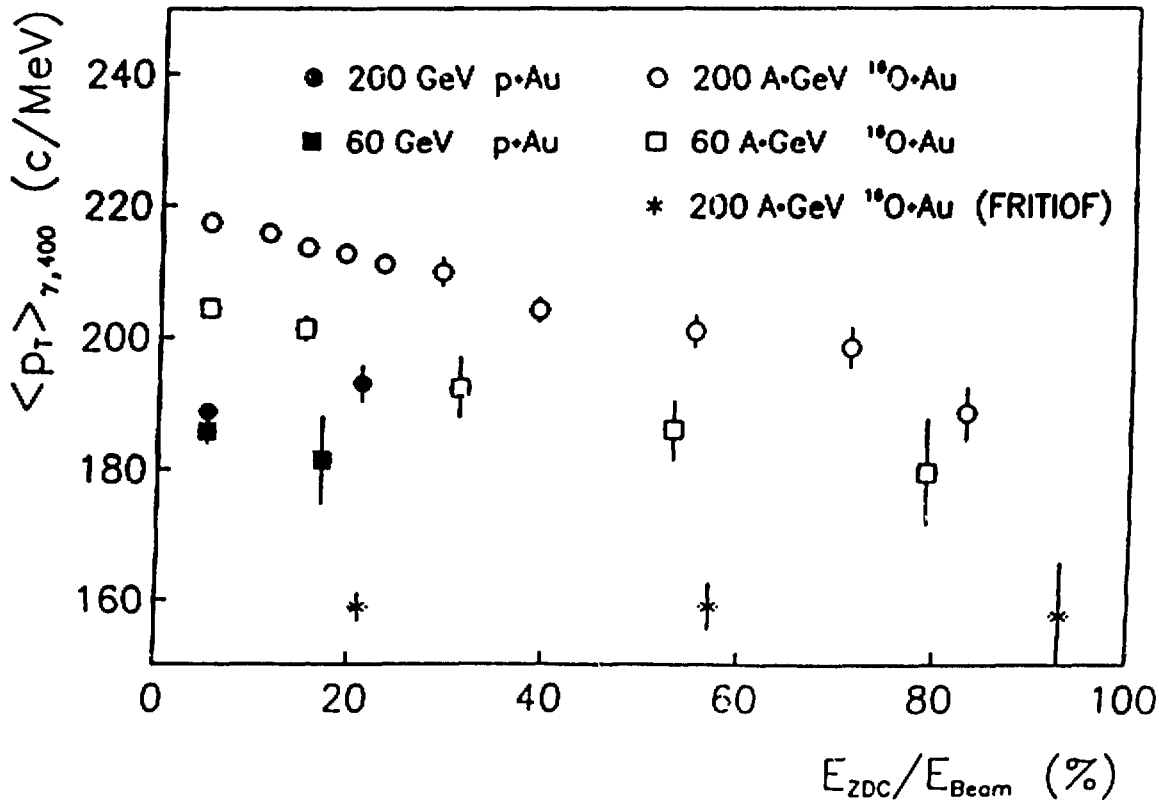

Fig. 9. Experimental $\langle p_T \rangle_{\gamma,400}$ for inclusive photons from the truncated p_T distributions (see text) as a function of centrality of the reaction defined by the energy deposited in the ZDC in percent of the beam energy.

For proton projectiles, E_{ZDC} is not a good measure of event centrality due to the strong effect of leading particles. Consequently, for appropriate comparisons of oxygen-induced and proton-induced reactions and for comparisons with thermodynamical models,[2] use is made of the entropy density,[2,19] which is proportional to $(dN/d\eta)A_{inc}^{-2/3}$. Here $dN/d\eta$ is the central multiplicity, approximated by the charged-particle multiplicity in the range $1.2 < \eta < 4.2$, multiplied by 1.5 to account for undetected neutral particles, and A_{inc} is the number of projectile participants derived from the ZDC spectrum via FRITIOF calculations in a procedure similar to that discussed in Section 5. The resulting plot of $\langle p_T \rangle_{\gamma,400}$ versus entropy density is shown in Fig. 10. At low values of the entropy density, a general increase of the average transverse momenta is observed for all systems. The $^{16}O + ^{197}Au$ data at 200 A GeV

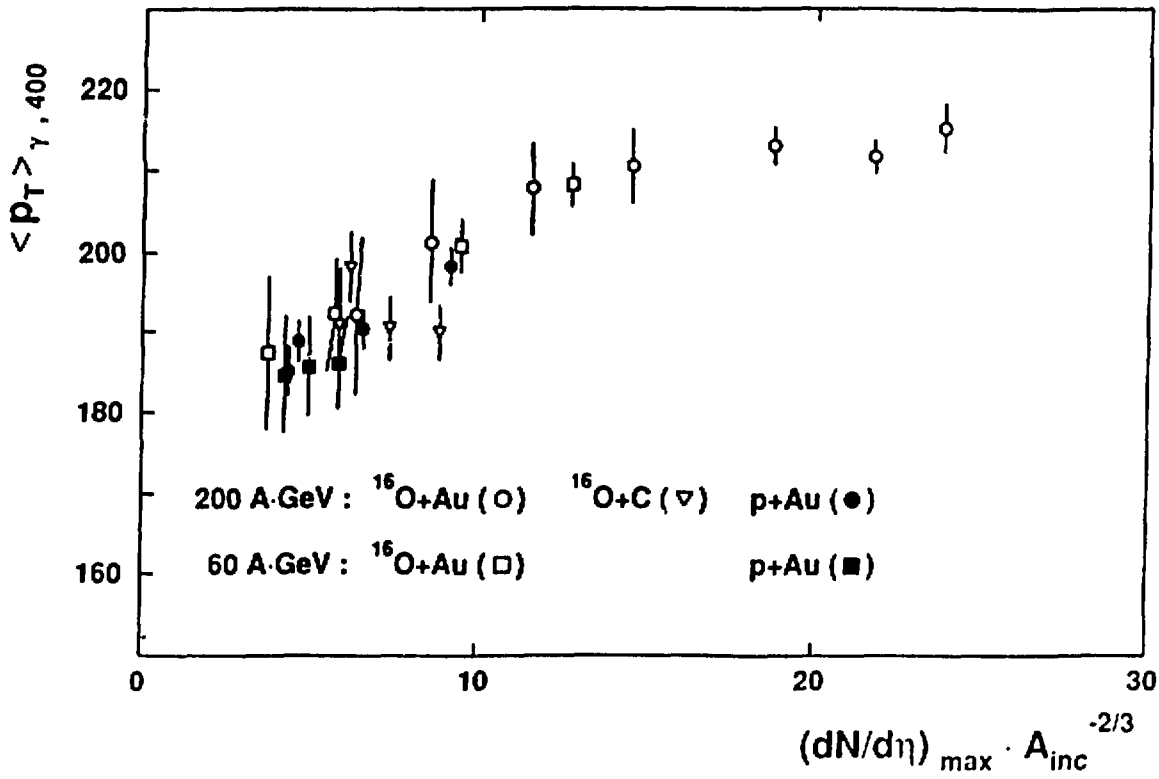

Fig. 10 Experimental $\langle p_T \rangle_{\gamma,400}$ for inclusive photons as a function of entropy density (see text).

extend to very high entropy density values, but the trend of increasing $\langle p_T \rangle_{\gamma,400}$ is not maintained. Instead, a large plateau is observed. Such a plateau, followed by a rise of $\langle p_T \rangle$ with increasing entropy density, was postulated by Van Hove[21] to be an indication of a phase transition to the quark-gluon plasma. The observation of an extended plateau in our case may be an indication of the formation of a mixed hadronic and plasma phase.

9. TARGET FRAGMENTATION

In this final section we discuss the nature of target spectator products. It is obvious that when the projectile is smaller than the target nucleus, target spectators contribute to the total reaction yield, regardless of the impact parameter. The various distributions of target spectator observables reflect the transparency of nuclear matter for an ultrarelativistic projectile. The Plastic Ball, which is a combination of a calorimeter and a charged-particle multiplicity detector, enables us to carry out unique studies of target spectator products. In particular, due to the particle-identification capabilities of the Plastic Ball (see Section 2), baryon distributions can be deduced. In Fig. 11 the average numbers of baryons per event detected in the Plastic Ball range ($-1.7 \leq \eta \leq 1.3$) are shown as a function of event centrality, which is determined by the energy observed in the ZDC. The baryon numbers are corrected for multiple hits and for neutrons, which are not detected in the Plastic Ball. The shaded band denotes systematic errors associated with the identification of high-energy protons. The striking feature is the fact that for the most central collisions, the total number of measured baryons in this target rapidity region amounts to approximately the total number of baryons of the initial colliding systems, excluding the baryons that are involved in the participant zone. This implies that, for central collisions, the transferred energy is sufficiently high to cause the complete disintegration of the target into particles with $Z \leq 2$. With decreasing collision centrality, an increasing number of low-energy

fragments with Z > 2 are produced. These particles are not identified by the Plastic Ball but have been observed by other techniques.[20,21]

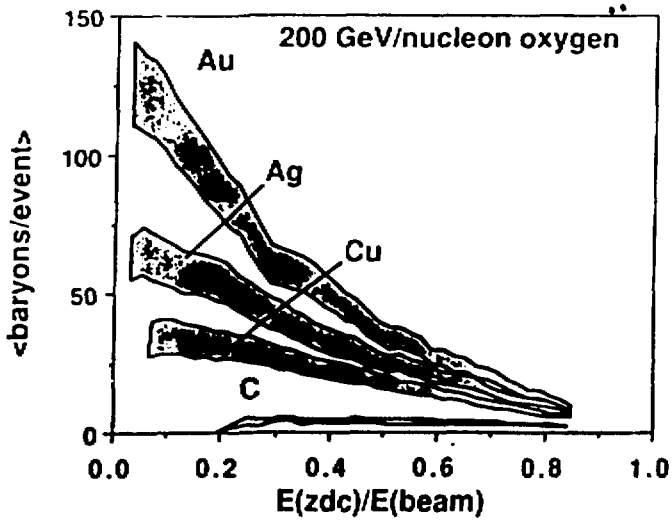

Fig. 11. Average number of baryons per event from reactions induced with 200 A GeV ^{16}O as a function of collision centrality, which is determined by the energy measured in ZDC. The measurements were made with the Plastic Ball in the pseudorapidity range $-1.7 < \eta < 1.3$, and a correction has been applied to the data to account for neutrons, which are not detected by the Ball. The shaded bands denote uncertainties in the identification of high-energy protons.

Distributions of baryons as a function of pseudorapidity for central collisions of ^{16}O at 60 and 200 A GeV and of protons at 200 GeV with various targets is shown in Fig. 12. The proton distributions have been multiplied by the A/Z ratio of the target to account for the undetected neutrons. The pseudorapidity distributions shown are essentially equivalent to angular distributions, and differ significantly from actual rapidity distributions. For the O + Au reactions, the shape of the distributions in Fig. 12 is similar for all targets at both energies. The magnitude is proportional to the target mass. The shape observed is a result of the "drag" of the target baryons to the forward direction. We conclude that a sizable fraction of the target baryons — the participating baryons — must appear beyond the range of the Plastic Ball, at $\eta > 1.3$. In contrast, in the absence of a similar

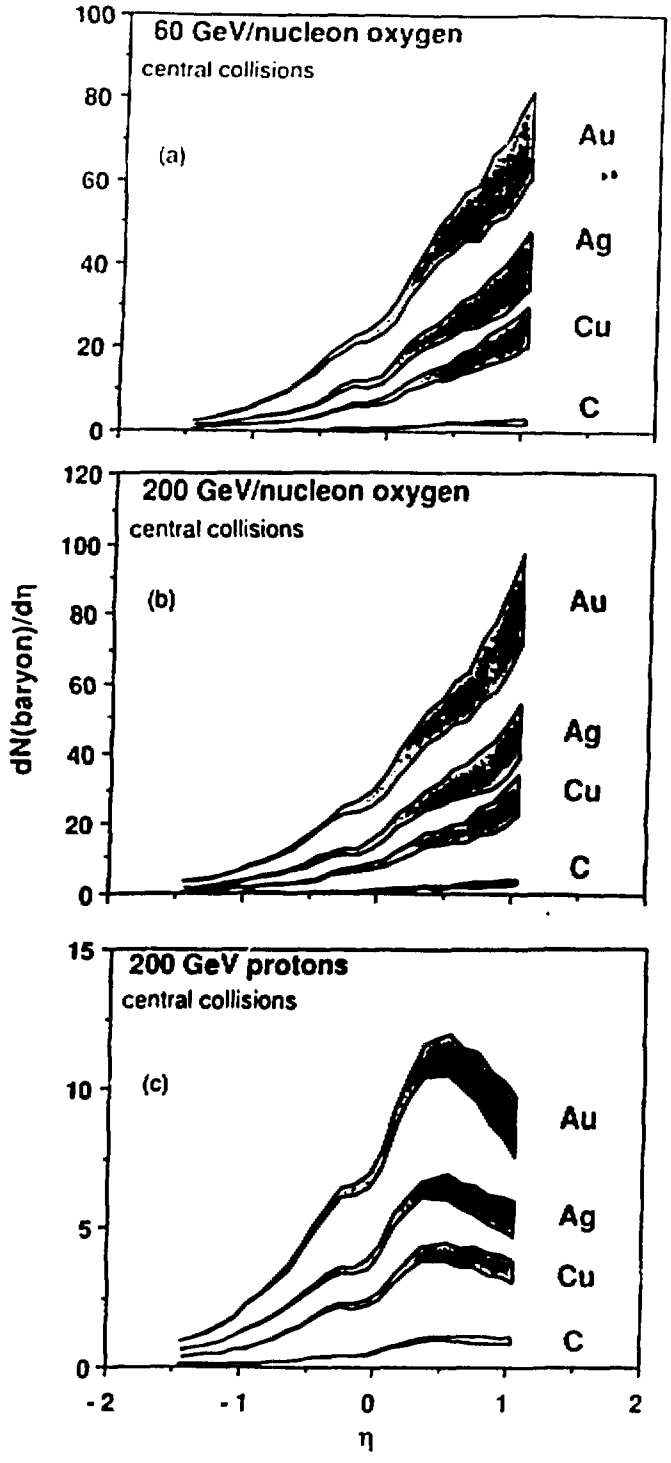

Fig. 12. Average number of baryons per event as a function of pseudorapidity for central collisions of ^{16}O and proton projectiles with various target nuclei. The numbers shown were measured with the Plastic Ball and multiplied by the A/Z ratio of the target to account for undetected neutrons. The shaded bands denote uncertainties in the identification of high-energy protons.

"drag," the shapes of the p + A distributions exhibit a clear maximum within the Plastic Ball range, at a pseudorapidity of about 0.5.

Transverse energies of particles emitted from a common source relate to the temperature of the source. The average transverse energy of protons measured by the Plastic Ball rises from 50 MeV at $\eta \approx -1.5$ to a peak at about 200 MeV at $\eta \approx 0.9$. The transverse energy values in the region of the peak ($0.6 < \eta < 1.0$) are plotted in Fig. 13 for 200 GeV A $^{16}O + ^{197}Au$ as a function of event centrality. The width of the band again respresents the uncertainty associated with high-energy proton identification. It can be seen that in very central events, the average proton transverse energy is ≈175 MeV. In contrast, at Bevalac energies ranging from 150 to 800 MeV/nucleon, in Au + Au collisions at $y_{cm} = 0$, the observed mean transverse proton energies do not exceed 160 MeV.[22] The surprising conclusion from this comparison is that the target spectator matter in ultrarelativistic heavy-ion collisions is highly excited and that the degree of excitation is similar to that of the participant fireball matter created in central collisions of very heavy nuclei in the energy range near 1 GeV/nucleon.

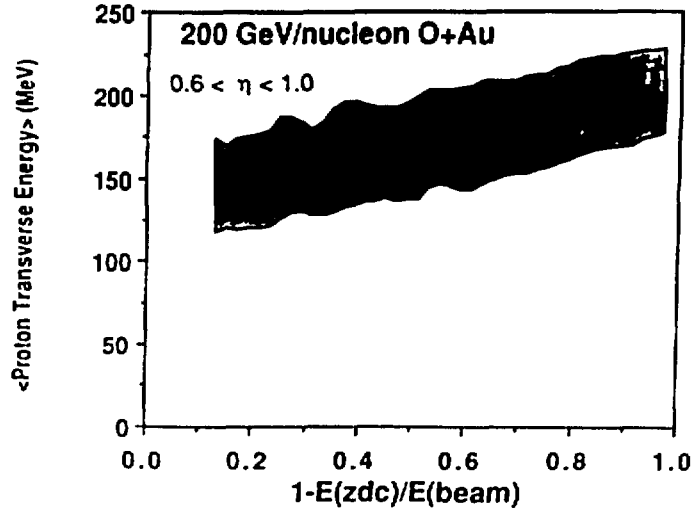

Fig. 13. Average transverse energy of protons from 200 A GeV ^{16}O interactions with Au measured in the pseudorapidity range $0.6 < \eta < 1.0$ as a function of collision centrality, determined by the energy deposited in the ZDC.

10. CONCLUSION

In summary, we have stressed the importance of nuclear geometry in nucleus-nucleus collisions at ultrarelativistic energies. We have presented forward and transverse energy measurements and have used the results to deduce the average number of participating nucleons, the degree of nuclear stopping, and the range of attained energy densities. The average transverse energy per participating nucleon at a given bombarding energy was found to be nearly independent of target mass and was found to vary only slowly with collision centrality. The degree of nuclear stopping for $^{16}O + ^{197}Au$ at 200 A GeV was found to be in the range of 25-60%, depending on the specific definition of stopping. Typical estimates of volume-averaged energy densities range from 1.8 to 2.4 GeV/fm^3. Higher energy densities are predicted to be attained in the core region of very large colliding systems.

Inclusive photon transverse momentum distributions were presented and discussed. Significant deviations from the FRITIOF model were noted. Extracted slope parameters were found to be in the range of 180 to 240 MeV/c. The plot of the average transverse momentum was found to exhibit a large plateau in the case of $^{16}O + ^{197}Au$ at 200 A GeV, which could be attributed to the onset of a mixed plasma and hadronic phase. Target fragmentation products were found to be highly excited and showed evidence of "drag." The excitation of target spectators at 200 A GeV was found to be comparable to that of the participant fireball at 1 A GeV. The results presented here, together with our charged-particle multiplcility results,[10] provide us with a reasonably comprehensive survey of interactions of ^{16}O with various target nuclei in the energy range from 960 GeV to 3.2 TeV.

REFERENCES

[1] See, for example, Proc. Third Int. Conf. on Ultrarelativistic Nucleus-Nucleus Collisions, Brookhaven National Laboratory, Upton, N.Y., U.S.A., 1983, eds. T. Ludlam and H. Wegner, Nucl. Phys. A418 (1984); Proc. Fourth Int. Conf. on Ultrarelativistic Nucleus-Nucleus Collisions, Helsinki, Finland, 1984, ed. K. Kajantie, Lecture Notes in Physics 221 (1984) (Springer, Berlin, 1984); Proc. Fifth Int. Conf. on Ultrarelativistic Nucleus-Nucleus Collisions, Asilomar, California, U.S.A., 1986, eds. L. S. Schroeder and M. Gyulassy, Nucl. Phys. A461 (1987); L. McLerran, Rev. Mod. Phys. 58, 1021 (1986) and references therein.

[2] Van Hove, L., Nucl. Phys. A447, 443c (1985).

[3] Albrecht, R., et al., Phys. Lett. 199B, 297 (1988).

[4] Sorensen, S. P., et al., Z. Phys. C 38, 3 (1988).

[5] Albrecht, R., et al., Phys. Lett. 202B, 598 (1988).

[6] Lund, I., et al., Z. Phys. C 38, 51 (1988).

[7] Albrecht, R., et al., Phys. Lett. 201B, 390 (1988).

[8] Loehner, H., et al., Z. Phys. C 38, 97 (1988).

[9] Schmidt, H. R., et al., Z. Phys. C 38, 109 (1988).

[10] Otterlund, I., et al., proceedings of this conference.

[11] Nilsson-Almqvist, B., and E. Stenlund, Comput. Phys. Commun. 43, 387 (1987); B. Andersson et al., Phys. Rep. 97, 31 (1983); Phys. Scr. 34 451 (1986); Lund University Report LU-TP 86-3 (Lund, Sweden, (1986).

[12] Albrecht, R., et al., Report GSI-85-32, Gesellschaft fuer Schwerionenforschung, D-6100 Darmstadt, West Germany (August 1985).

[13] Gutbrod, H. H., et al., Proc. Int. Workshop on Gross Properties of Nuclei and Nuclear Excitations XV, Hirschegg, Austria, 1987, ed. Hans Feldmeier, GSI and Institut fuer Kernphysik, Darmstadt, 1987, p. 42.

[14] Baden, A., et al., Nucl. Instrum. Methods 203, 189 (1982).

[15] Bamberger, A., et al., Phys. Lett. 184B, 271 (1987).

[16] Franz, A., "The Transverse Energy Flow in Hadron-Lead Collisions at 200 GeV/c Incoming Momentum," Ph.D. Thesis, University of Siegen (1986).

[17] Abbott, T., et al., Phys. Lett. 197B, 285 (1987).

[18] Corriveau, F., et al., Z. Phys. C 38, 15 (1988); T. Åkesson et al., to be published in Z. Phys. C.

[19] Bjorken, J. D., Phys. Rev. D 27, 140 (1983).

[20] Berthier, B., et al., Phys. Lett. 193B, 417 (1987).

[21] Aleklett, K., L. Sihver, and W. Loveland, Phys. Lett. 197B, 34 (1987).

[22] Doss, K.G.R., et al, submitted to Mod. Phys. Lett.; K. H. Kampert in Proc. 8th High-Energy Heavy-Ion Study, Lawrence Berkeley Laboratory, Berkeley, California, U.S.A., 1987, Report LBL-24580, p. 154.